A METHOD FOR MEASUREMENT OF HYDRAULIC LOSSES IN CENTRIFUGAL PUMPS

Cleber Sandim Ximenes
State University of Campinas – UNICAMP-FEM-DEP – Cx.P. 6122 - 13083-970 – Campinas, SP, Brazil
ximenes@dep.fem.unicamp.br

Antonio Carlos Bannwart
State University of Campinas – UNICAMP-FEM-DEP – Cx.P. 6122 - 13083-970 – Campinas, SP, Brazil
bannwart@dep.fem.unicamp.br

Fernando A. França
State University of Campinas – UNICAMP-FEM-DE – Cx.P. 6122 - 13083-970 – Campinas, SP, Brazil
ffranca@fem.unicamp.br

Valdir Estevam
PETROBRAS – E&P – Rio de Janeiro, RJ, Brazil
vestevam@petrobras.com.br

Abstract. *The selection of a centrifugal pump for an ESSP application depends on many factors, including fluid properties such as viscosity and density. When a centrifugal pump is handling a viscous fluid - such as heavy oil - its performance is impaired in comparison to operation with light oils due to increased frictional losses. There are very few published data available to evaluate the magnitude of viscous effects. Usually the performance decay for operation with viscous fluids is estimated by means of empirical correction factors applicable to flow rate, head and efficiency. However, large discrepancies between actual and predicted performance have been observed in practice. The current work has as objective to develop a method for measurement and evaluation of the losses in centrifugal pumps. This is carried out by employing one-dimensional balance equations for the single-phase flow into the pump. Focus is directed to the hydraulic losses, which include frictional, recirculation and shock losses. Measurements performed with water in a two-stage pump at several Reynolds numbers and rotation speeds are presented and discussed.*

Keywords: *Petroleum engineering, heavy oil, centrifugal pumps, electrical submersible pumps, viscous effects.*

1. Introduction

The viability of heavy oil production in offshore deep and ultra-deep water fields depends upon the development and improvement of artificial lift methods, among which the Electrical Submersible Submarine Pump (ESSP) has been demonstrated to be an important method for high flow rate wells. The selection of a centrifugal pump for use in an ESSP application depends, of course, on its performance parameters. Typical performance curves are shown in Fig. 1, which illustrates the relationships between pump head, pump efficiency and break horsepower, with the liquid flow rate. The manufacturer usually provides these experimentally determined curves using water. The performance curves are extremely dependent upon the pump impeller and diffuser's geometric design.

As sketched in Fig. 2, a typical single-stage pump consists of an impeller rotating within a casing. The fluid enters axially through the eye of the casing, it is caught up in the impeller blades and whirled tangentially and radially outward until it leaves through all circumferential parts of the impeller into the diffuser part of the casing. The fluid gains both velocity and pressure while passing through the impeller. The diffuser or scroll section of the casing decelerates the flow and further increases the pressure.

The top view of a typical impeller is illustrated in Fig. 3. A generic sketch of a radial impeller is shown in Fig. 4. The impeller rotates clockwise with the pump shaft angular velocity, ω. The diffuser is stationary. The inside circle is the entrance of the impeller, or discharge of a diffuser. The outside circle is the discharge of the impeller, or entrance of a diffuser. The impeller or diffuser is divided into several channels by curves blades. The angle β between the outward blade tangent and the peripheral line opposing the rotating direction is called the blade angle at that location. By convention, the subscript 1 refers to entrance, while subscribe 2 refers to discharge. Therefore, for the impeller shown in Fig. 4, β_1 is the impeller entrance blade angle and β_2 is the impeller discharge blade angle. The dashed curve at the middle of the channel is called the streamline of fluids, if the flow inside the channel is assumed to be one-dimensional.

Performance curves based on water tests supply realistic values to efficiency, head and capacity (flow rate) when the fluid has a viscosity that is about the same as water (1 cP). In many cases, however, the liquid pumped (such as viscous oil, sugar mollases, etc) may be more viscous. In these cases, pump performance considerably changes from behavior shown by the actual measurement with water. Viscous liquids cause greater hydraulic losses in the pump, leading to lower pumping head and efficiency and greater power. The pumping head and pumping efficiency curves fall below the corresponding water-performance curves, while the shut-off head point remains the same, regardless the viscosity.

The correction factors published by the Hydraulic Institute (HI) are widely used to predict the performance of a centrifugal pump with viscous fluids. When the characteristics for pumping water is known, those for a viscous liquid can be determined by multiplying the water values by correction factor to head, efficiency and capacity. The corrections factors provide by HI are a conclusion based on tests of conventional centrifugal pumps with petroleum oils. Nevertheless, in many cases, the correction method of HI gives a pessimistic prediction of pump performance and therefore tremendous over sizing that can take to an impractical project. Although fluid viscosity is very decisive on centrifugal pump applications, there are few publications about centrifugal pumps handling high-viscosity fluids.

Wen-Guang Li (2002) presents a method for determining some parameters, such as slip factor, hydraulic, mechanical and volumetric efficiencies based on the experimental performance of centrifugal oil pumps. The investigation was performed with a single-stage centrifugal pump handling fluids with kinematical viscosity range among 1 cSt and 255 cSt. Comparisons between prediction and test data were done. The experimental results demonstrated that mechanical and hydraulic efficiencies decrease as the viscosity of liquid pumped increases, in contrast with volumetric efficiency that has nothing to do with viscosity variation.

Recently, Gülich (2003) revealed that disk friction and friction losses in the hydraulic passages of the pump are the dominating factors. In these investigations a mathematical model based on an analysis of the viscous losses in the centrifugal pump was developed.

However, it is important to point out that the research groups cited previously present correlations valid for the specific pump designs tested. In the present work, a laboratory scale apparatus was used to investigate and to formulate a generic model for fluid flow through centrifugal pump.

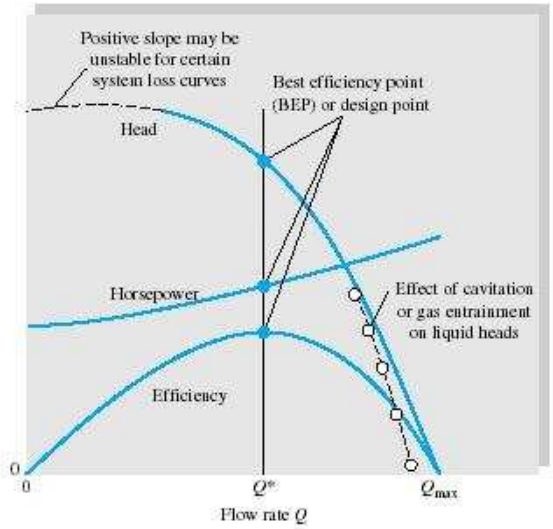

Figure 1: Typical centrifugal pump performance at constant impeller rotation speed (White, 1994).

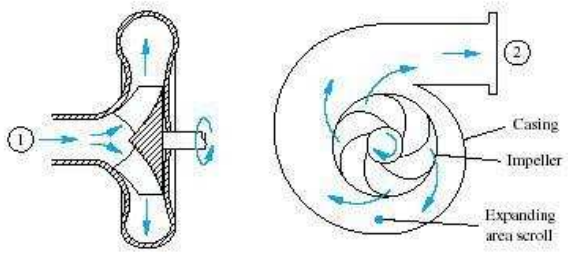

Figure 2: Typical centrifugal pump

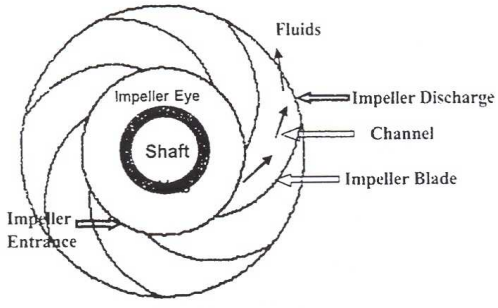

Figure 3: Impeller top view

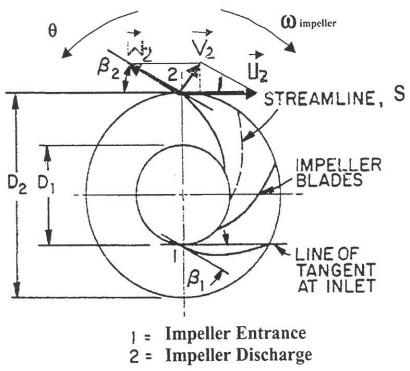

Figure 4: Sketch of a radial impeller's geometry

2. One-dimensional approach

2.1. Fluid velocity and central streamline

The velocity field inside the channel is three dimensional and very complexes. In this study, one-dimensional flow along a channel is assumed based on continuity, linear momentum, angular momentum and energy equations. The fluids

particles flow along a streamline as shown in Fig. 5. The relative velocity, ***w,*** between the fluids and the channel is tangent to the central streamline. The flow area is normal to the streamline. The fluids flow from the entrance to the discharge of the impeller along each curved channel. During this operation, the impeller is rotating around the shaft axis, and any point on the impeller has a peripheral velocity, ***u*** given by,

$$u = \omega r \tag{1}$$

where $\boldsymbol{\omega}$ is the angular velocity of the rotating shaft or impeller in the clockwise direction, and ***r*** is the radial position of a point on the impeller. The fluid particle has absolute flow velocity, ***V,*** that is the vectorial sum of the relative velocity of the flow and the peripheral velocity,

$$V = w + u \tag{2}$$

The diagram for the velocity vectors is shown in Fig. 4. This is called the velocity triangle diagram. The angle $\boldsymbol{\beta_i}$ between $\boldsymbol{w_i}$ and the negative of $\boldsymbol{u_i}$, and in ideal flow case the same as the angle between the tangent to the impeller channel and a line in the direction of motion of the vane. $\boldsymbol{V_{ni}}$ and $\boldsymbol{V_{ti}}$ are, respectively, the radial and tangential components of the absolute velocity, $\boldsymbol{V}$. Relationships between these velocities and their components can be obtained from simple geometric relations. For ideal, one-dimensional, one-phase flow through a pump, the velocity triangles are a function of the pump geometry, angular impeller velocity and the mass flow rate.

For stead-state, one dimensional and incompressible flow, the equation of continuity, linear momentum, angular momentum and energy applied between the inlet and outlet of the impeller reduces to (see Nomenclature section):

- *Mass Conservation Equation*

$$Q = 2\pi r_1 b_1 V_{n1} = 2\pi r_2 b_2 V_{n2} \tag{3}$$

- *Linear Momentum Conservation Equation*

$$\left(\frac{p_1}{\rho g} + \frac{w_1^2}{2g} + z_1 - \frac{u_1^2}{2g}\right) - \left(\frac{p_2}{\rho g} + \frac{w_2^2}{2g} + z_2 - \frac{u_2^2}{2g}\right) = \int_1^2 \frac{\tau_w S_w ds}{\rho g A} + h_{i,local} \tag{4}$$

where $\boldsymbol{h_{i,local}}$ stands for the local irreversible losses that can be associated mainly with flow separation.

- *Angular Momentum Conservation Equation*

$$T_s - T_m = \rho Q\left(r_2 V_{t2} - r_1 V_{t1}\right) \tag{5}$$

- *Energy Conservation Equation*

$$H = h_s - h_f = \left(\frac{p_2}{\rho g} + \frac{V_2^2}{2g} + z_2\right) - \left(\frac{p_1}{\rho g} + \frac{V_1^2}{2g} + z_1\right) \tag{6}$$

A relationship among Eqs. (4-6) appears when Eq. (5) is multiplied by $\omega/(\rho Q g)$. The following result is obtained:

$$h_s = \frac{u_2 V_{t2} - u_1 V_{t1}}{g} \tag{7}$$

where $h_s = \dfrac{(T_s - T_m)\omega}{\rho Q g}$ is the head supplied by the pump. Additional insight is gained by rewriting these relations in another form when velocity triangle is applied:

$$uV_t = \tfrac{1}{2}\left(V^2 + u^2 - w^2\right) \tag{8}$$

Replacing Eq. (8) into Eq. (7) reads:

$$h_s = \frac{1}{2g}\left[\left(V_2^2 + u_2^2 - w_2^2\right) - \left(V_1^2 + u_1^2 - w_1^2\right)\right] \tag{9}$$

Inserting Eq. (9) into (6) gives the following result:

$$\left(\frac{p_1}{\rho g}+\frac{w_1^2}{2g}+z_1-\frac{u_1^2}{2g}\right)-\left(\frac{p_2}{\rho g}+\frac{w_2^2}{2g}+z_2-\frac{u_2^2}{2g}\right)=h_f \tag{10}$$

Equations (10) and (4) become equivalent if:

$$h_f=\int_1^2\frac{\tau_w S_w ds}{\rho g A}+h_{i,local} \tag{11}$$

According to Stephanoff (1957) the hydraulic losses are, in a one-dimensional approach, not only the least well known, but also the most important. Hydraulic losses can be roughly categorized as friction, eddy and separation losses caused by changes in direction and magnitude of the velocity (including the shock and diffusion loss). Thus, $\boldsymbol{h_f}$ must include all irreversibilities associated with wall friction, recirculation and shocks of the flow through the impeller. In this work, Eq. (10) is used to experimentally determine $\boldsymbol{h_f}$.

The theoretical head, $\boldsymbol{h_s}$, supplied to the fluid can be expressed by a different version of Eq. (7), i.e.:

$$h_s=\frac{1}{g}\left[u_2\left(u_2-V_{n2}\cot\beta_2\right)-u_1\left(u_1-V_{n1}\cot\beta_1\right)\right]=\frac{1}{g}\left[u_2\left(u_2-u_2V_{n2}\cot\beta_2\right)-u_1V_{n1}\cot\alpha_1\right] \tag{12}$$

The net head, $\boldsymbol{H}$, results from the difference $\boldsymbol{h_s - h_f}$. For completeness, we introduce the overall efficiency, $\boldsymbol{\eta}$, which is the ratio of the power delivered by the pump to the fluid to the power absorbed by the pump. This parameter is basically composed of three terms: mechanical, hydraulic and volumetric efficiencies. If $\boldsymbol{h_f}$ is known, then the hydraulic efficiency can be obtained as:

$$\eta_h=\frac{H}{h_s}=1-\frac{h_f}{h_s} \tag{13}$$

Besides the head losses, there are capacity losses known as leakage losses. The ratio between the capacity available at the pump discharge, $\boldsymbol{Q}$, and that passing through the impeller, $\boldsymbol{Q+Q_L}$, is known as volumetric efficiency:

$$\eta_V=\frac{Q}{Q+Q_L} \tag{14}$$

Mechanical losses include those due to the stuffing box and those at the bearings. These losses, according to Stephanoff (1957), are relatively small compared to other losses and arise due to the design of the ball bearings and the stuffing box. They can be related to the mechanical efficiency by:

$$\eta_m=\frac{\dot{W}_s-\dot{W}_m}{\dot{W}_s}=\frac{(T_s-T_m)\omega}{T_s\omega}=1-\frac{T_m}{T_s} \tag{15}$$

The relationship among the partial efficiencies and the overall efficiency can be obtained from:

$$\eta=\frac{\rho QgH}{T_s\omega}=\eta_m\eta_h\eta_v \tag{16}$$

3. Experimental work

The experimental results presented in this paper were obtained in the Multilab Facility at the School of Mechanical Engineering of UNICAMP. The experimental apparatus is illustrated in Fig. 5. The closed-loop circuit is composed by: a 2-stage test pump Ita 65-330/2 supplied with an 5 hp electric motor and shaft speed of 1200 rpm, a booster single-stage pump Ita 65-160 provided with an 5 hp electric motor and shaft speed of 1750 rpm, a shaft speed controller for booster and test pumps, a digital torque meter connected between electric motor and test pump axis, pressure sensors at specific points of the test pump, magnetic and vortex flow meters, globe and sphere valves for flow control, and a 5 m^3 capacity reservoir. Table 1 lists the geometric data of the test pump impellers.

Performance data were recorded using tap water. Flow rate, suction pressure, 1st stage exit pressure, discharge pressure, shaft torque, and shaft speed were measured. Fig. 6 presents schematically the locations of the pressure sensors into the pump. In the experimental procedure the booster pump worked with its maximum rotation fixed in 1750 rpm. Shaft speeds of 600, 700, 800, 900 and 1000 rpm were established to test pump by means shaft speed controller. For each one of these rotations, at least ten data were collected between shut off and maximum flow rate (38 m^3/h) for

each of the characteristic curves. Vortex and magnetic meters controlled by means of a sphere valve set in the discharge line were used for flow rate measurement. These data were used to determine the net head of each impeller, the pump net head, the input shaft power and the head loss between inlet and outlet of each impeller, for each test run.

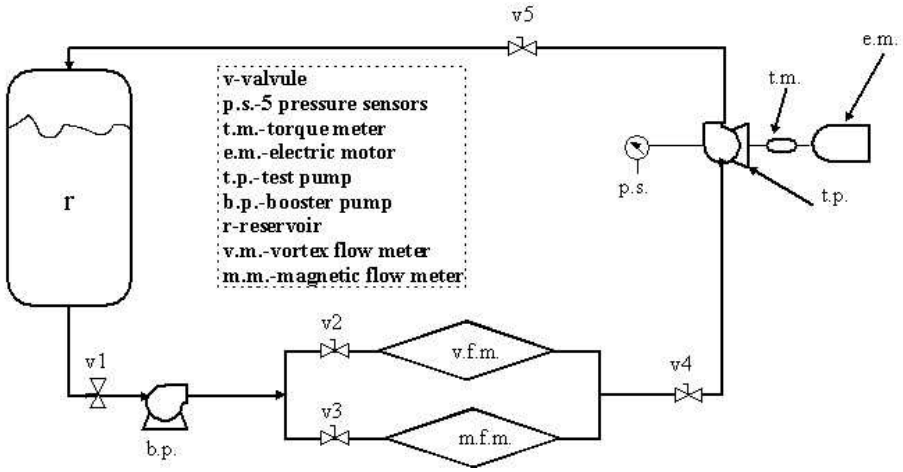

Figure 5: Sketch of closed circuit

Table 1: Input geometric data for the impeller

	1st impeller	2nd impeller
Number of blades (N)	8	8
Blade thickness (δ)	3mm	4mm
Channel width at inlet (b_1)	21mm	21mm
Impeller entrance diameter (D_1)	80mm	76mm
Impeller discharge diameter (D_2)	205mm	260mm
Inlet blade anlge (β1)	20°	20°
Oultet blade angle (β2)	35°	35°

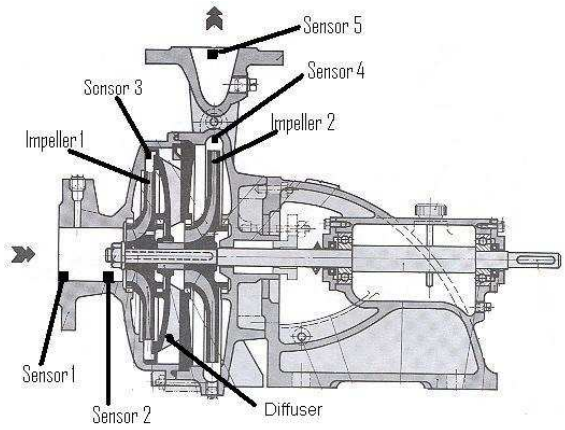

Figure 6: Points where pressure sensors were placed into the pump

4. Results

In order to assess the proposed measurement method, the net pump head, ***H***, is plotted against the flow rate in Fig. 7, for several pump rotation speeds. This is, perhaps, the most typical characteristic curve of centrifugal pumps. It can be observed that the net head increases with increasing pump speed and decreases with increasing flow rates, as expected.

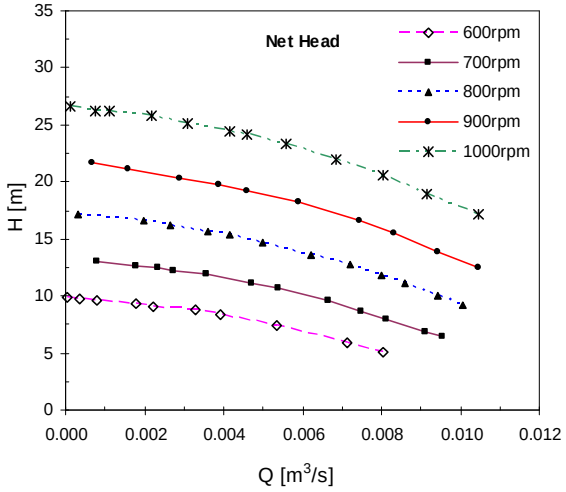

Figure 7. Net pump head

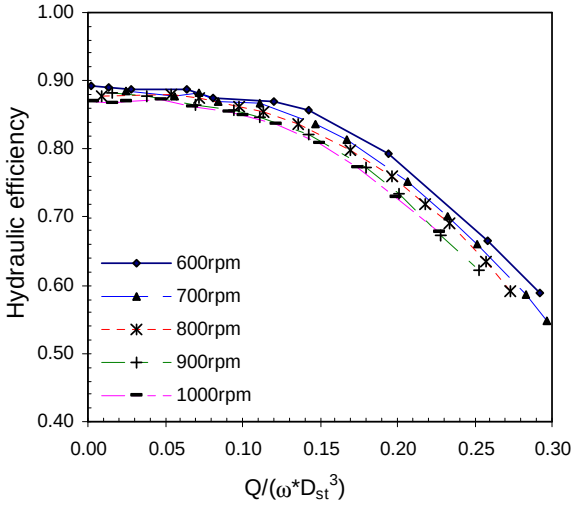

Figure 8: Hydraulic efficiency

The hydraulic efficiency η_h is shown in Fig. 8 as a function of the capacity coefficient, $Q/\left(\omega D_{st}{}^3\right)$ at several pump rotation speeds. As can be observed, the constant pump speed curves are all very close, confirming the validity of the similarity rules derived from dimensional analysis. It is also important to note that the hydraulic efficiency does not vanish at shut off, since the fluid keeps being pressurized.

Figures 9 and 10 show the hydraulic head losses, h_f, for each impeller, as a function of the Reynolds number at different pump speeds. The Reynolds in each impeller channel was defined by $Re = \rho \overline{V}_n \overline{D}_h / \mu$, where $\overline{D}_h$ is the average hydraulic diameter between the inlet and outlet of each impeller, defined as $\overline{D}_h = 4(bC)/[2(b+C)]$ and $C = 2\pi r/N - \delta$, and $\overline{V}_n$ is the average flow velocity relatives to the impeller. Both figures show that the head losses increase with increasing Reynolds number, which means that the losses increase with increasing flow rates. However, the constant speed curves are neatly apart from each other for the second impeller, which also presents higher losses in comparison with the first impeller. This can be due to the different nature of the flow arriving at each stage, and also to the greater discharge diameter of the second impeller, which causes more recirculation (i.e. flow separation) in comparison with the first impeller. Note also that the head loss does not vanish at shut off, indicating the presence of other types of loss that do not depend of flow rate, such as shocks and recirculation.

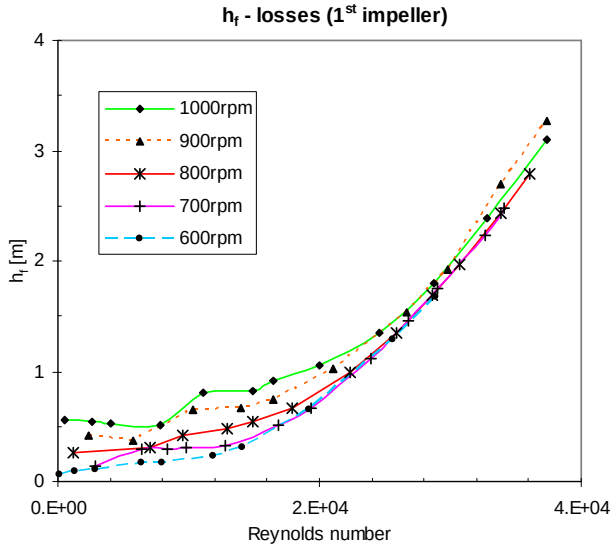

Figure 9: Head lost by fluid between inlet and outlet into the first impeller

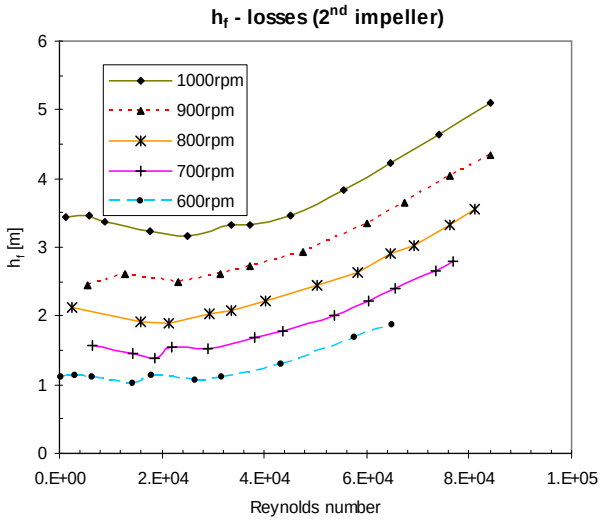

Figure 10: Head lost by fluid between inlet and outlet into the second impeller

Figure 11 for the first impeller and Fig. 12 for the second one show the dimensionless head loss $h_f/\left(\overline{w}^2/2g\right)$ as a function of the Reynolds number for several rotation speeds. It can be observed that, at a given rotation speed, the dimensionless head loss decreases as the Reynolds number increases, as for a pipe friction factor. This demonstrates the adequacy of the Reynolds number definition adopted, making clear the effect of fluid viscosity and density on the pump performance. Also, the dimensionless head loss increases with the rotation speed, which presumably causes an increase in the turbulence and recirculation. Hence, a tentative model for h_f in a single impeller can be suggested:

$$h_f = \underbrace{f_{channel}\left(Re, \frac{e}{D}, \frac{\omega D^3}{Q}\right)\frac{L_{channel}}{D_h{}^{av}}\frac{\overline{w}^2}{2g}}_{distribuited\ \ losses} + \underbrace{k_1\frac{(w_1 - w_2)^2}{2g}}_{recirculation\ \ losses} + \underbrace{k_2\frac{(w_1 - u_1/\cos\beta_1)^2}{2g}}_{shock\ \ losses} \qquad (17)$$

where the friction factor f and the parameters k_1 and k_2 can be, in principle, determined from h_f data. Note that at zero flow rate (shut-off) the two first terms on the R.H.S. of Eq. (17) vanish, whereas the third one depend on the square of rotation speed. This agrees with the previous comments regarding Figs. 9 and 10. The low range of Reynolds number data does not allow for the moment to determine if k_1 and k_2 depend on Reynolds number and pump rotation or not.

5. Conclusions

This study presents a method to measuring hydraulic losses in centrifugal pumps. The method is based on the one-dimensional balance equations for mass, linear momentum, angular momentum and energy.

Data collected in a two-stage pump working with water indicate that the hydraulic efficiency decreases with the flow capacity coefficient and the hydraulic losses increase with flow rate.

When expressed in dimensionless form, these losses become equivalent to a friction factor, decreasing as the channel Reynolds number increases. This makes clear the effect of fluid properties (viscosity and density) on the pump perfomance. A tentative model for the evaluation of hydraulic losses is proposed, but more data in the low Reynolds number regions is necessary for validation.

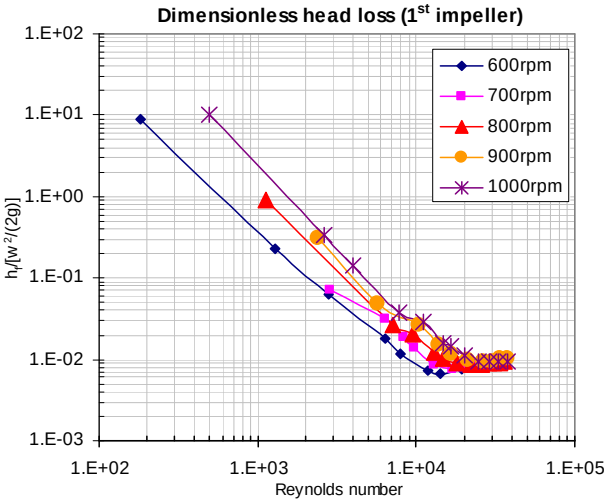

Figure 11: Dimensionless head losses by fluid between inlet and outlet into the first impeller

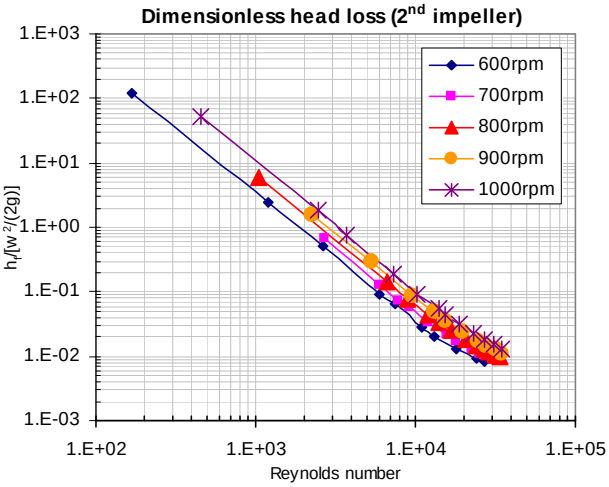

Figure 12:Dimensionless head losses by fluid between inlet and outlet into the second impeller

6. Nomenclature

Symbol	Description	Symbol	Description
b	blade width of impeller, m	p	pressure, Pa
r	radial position of a point on the impeller, m	H	net pump head, m
A	cross sectional area of channel $(A = 2\pi r b)$, m	h_s	theoretical head supplied to the fluid, m
z	difference between inlet and outlet of impeller, m	h_f	head lost by fluid between inlet and outlet of impeller, m
s	distance from the impeller entrance tip or the diffuser entrance tip to certain location on the streamline, m	$\dot{W}_s$	break horsepower (ωT_s), W
τ_w	shear stress on the average section, N/m^2	$\dot{W}_m$	mechanical power loss (ωTm), W
S_w	wetted perimeters of fluid on the channel cross-section, m	η_m	mechanical efficiency
T_s	impeller shaft torque, N.m	β	blade angle
T_m	impeller friction torque, N.m	ρ	density fluid, kg/m^3
V	absolute fluid velocity, m/s	V_t	absolute tangential fluid velocity, m/s
V_n	radial fluid velocity, m/s	w	fluid velocity relative to impeller channel, m/s
u	peripheral velocity (ω.r), m/s	Q	flow rate, m^3/s
g	acceleration of gravity, (9.8m/s^2)	S_w	wetted perimeter, m
ω	angular velocity, radians/s	Q_L	leakage flow rate
η_h	hydraulic efficiency	η_V	volumetric efficiency
$\overline{D}_h$	average hydraulic diameter, m	C	arc length, m
$\overline{V}_n$	average radial velocity between the inlet and outlet of channel, m/s	K	loss coefficient due to minor losses
$L_{channel}$	channel length, m	f_{curved}	friction factor to curved channels
w_o	relative velocity in the best efficiency point (BEP), m/s	dhl	dimensionless head losses (global friction factor)
D	impeller diameter, m		

Subscripts	Description		
st	first	nd	second
1	entrance	2	discharge

Acknowledgements

The authors thank ANP (Agencia Nacional do Petróleo), PETROBRAS and FINEP (Financiadora de Estudos e Projetos) for the financial support in different parts of this work.

References

American National Standard for Centrifugal Pumps.Hydraulic Institute, 1994, Parsippany.

Church, A. H., 1972, "Centrifugal Pumps and Blowers", Robert E. Krieger Publishing Company,USA, 308p.

Gülich, J. F., 2003, "Effect of Reynolds-number and surface roughness on the efficiency of centrifugal pumps", ASME Journal of Fluids Engineering, 125, 4, pp 670-679.

Stepanoff, A. J., 1957, "Centrifugal and Axial Flow Pumps", John Wiley & Sons, 2nd Edition, USA, 462 p.

Wen-Guang Li, Fa-Zhang Su, Cong Xiao, 2002, "Experimental Investigations of Performance of a Commercial Centrifugal Oil Pump", Transactions of the ASME, 124, pp 554-557.

White, F. M., 1994, "Fluid Mechanics", McGraw-Hill.

Responsibility notice

The authors are the only responsible for the printed material included in this paper.